Screening of Anti-Cancer Properties of Beta-Sitosterol and its Derivatives against Microtubules: Molecular Modeling Approach

Lakshminarayanan Karthik[1*], Balakrishnan Vijayakumar[2]

[1] Central Research Laboratory, Meenakshi Academy of Higher Education and Research, West K.K. Nagar, Chennai, Tamil Nadu, India – 600078

[2] São Carlos Institute of Physics (IFSC), University of São Paulo, Av. Joao Dagnone, 1100 – Jardim Santa Angelina, São Carlos 13563-120, Brazil.

ABSTRACT

A phytosterol compound, beta-sitosterol is found in abundance in many plants, fruits, and vegetables. They possess numerous health benefits and clinical uses including medicinal properties such as anti-diabetic, anti-atherogenic, anti-asthmatic, etc. The compound was also reported to possess anti-cancer property against various cancer cell lines. Microtubules which are hollow fibrous shafts and made up of tubulin protein play essential roles in cell division, cell movement and intracellular transport. Due to their major role in cell division, microtubules are considered as an attractive target for designing potent anti-cancer agents. Given their importance, the present study describes the molecular docking of beta-sitosterol and its analogs with the alpha/beta form of tubulin. For this, small molecule compounds structurally similar to beta-sitosterol were retrieved from PubChem and Binding databases. In the subsequent step, High Throughput Virtual screening was carried out with the tubulin-colchicine complex. Based on the virtual screening results and the nature of active site residues of the protein complex, the screened compounds were further taken to Induced Fit Docking studies using Schrodinger's GLIDE. Hydrogen bond interactions were analyzed between the compounds and active site amino acid residues. QikProp module and FAF-Drugs tools were used to analyze the pharmacokinetic properties of the selected compounds. Among the tested compounds, few compounds were found to satisfy all the *in silico* parameters and can be developed as potent inhibitors targeting microtubules.

Key Words: *Anti-cancer property; β-sitosterol; High Throughput Virtual Screening; Induced Fit Docking; Microtubules.*

eIJPPR 2020; 10(1):8-21

HOW TO CITE THIS ARTICLE: Lakshminarayanan Karthik, Balakrishnan Vijayakumar(2020). "Screening of Anti-Cancer Properties of Beta-Sitosterol and its Derivatives against Microtubules: Molecular Modeling Approach", International Journal of Pharmaceutical and Phytopharmacological Research, 10(1), pp.8-21.

INTRODUCTION

Phytochemicals found in many natural sources such as vegetables, fruits, and herbs are known to possess anti-cancer properties [1-3]. Beta-sitosterol (β-sitosterol) is one such phytochemical whose cancer-preventive properties are well documented in the previous studies [4]. A major plant sterol, β-sitosterol is found in fruits such as pomegranate, peanut, number of vegetables, olive oil, corn oil, avocado, and legumes [5, 6]. They were found to be effective against the colon and prostate cancer cell lines [7, 8] and also exhibited selective toxicity towards cancer cells without inducing considerable damage to normal cells [9]. In recent times, microtubules that form the cylindrical polymers of the protein tubulin has been considered an attractive drug target for designing potent anti-cancer compounds. Comprised of two non-identical subunits α and β, microtubules represent a major structural component of the cytoskeleton in eukaryotes. During cell division, the structural integrity of tubulin becomes essential as it

Corresponding author: Lakshminarayanan Karthik
Address: Central Research Laboratory, Meenakshi Academy of Higher Education and Research, West K. K. Nagar, Chennai - 600078
E-mail: ✉ lnbioinfokarthik @ gmail.com
Relevant conflicts of interest/financial disclosures: The authors declare that the research was conducted in the absence of any commercial or financial relationships that could be construed as a potential conflict of interest.
Received: 06 Aufust 2019 ; **Revised:** 17 December 2019 ; **Accepted:** 07 Janyary 2020

facilitates the formation of functional mitotic spindle resulting in proper segregation of sister chromosomes. The alpha/beta form of tubulin has become the target of numerous small-molecule ligands that interfere with microtubule dynamics aiding in cancer treatment [10].

Anticancer agents targeting microtubules are normally classified into two types viz., 'microtubule-stabilizing agents' (MSA) and 'microtubule destabilizing agents' (MDA). From the literature studies, it was observed that the dimer interface of the tubulin has remained the preferred binding site for MDAs such as noscapine [11] and indanocine [12, 13]. In particular, noscapine exhibited a stoichiometry of one molecule per tubulin dimer upon binding and resulted in altering the tubulin conformation. As for the indanocine, they were found effective against multidrug-resistant cancer cell lines and eliminated non-dividing cells without affecting the normal nonproliferating cells. These MDAs are reported to bind at this interface which has also been referred to as 'colchicine' or 'vinca' site (eg colchicine & vinblastine) and eventually resulting in cell death due to apoptosis. Moreover, most of the compounds projected as anti-cancer against microtubules are tested exclusively on this site [14]. As the existing anticancer drugs are presented with considerable drawbacks including toxic side effects, β-sitosterol appears to be a promising alternative. In this context, in the present study combined approaches of molecular modeling involving structure-based virtual screening followed by rigid and induced fit docking were performed to identify potent analogs of β-sitosterol. Based on scoring function the best possible inhibitors were identified and to determine the drug-likeness and reactivity, their Absorption, Distribution, Metabolism, Excretion, and Toxicity (ADMET) properties and cytotoxicity effects on various cancer cell lines were also evaluated. The combined computational approaches described the β-sitosterol derivatives can be expected to be useful in the development of potent anti-cancerous agents.

MATERIALS AND METHODS

Protein Preparation

The crystal structure of a heterodimer tubulin-colchicine complex was retrieved from Protein Data Bank (PDB ID: 1SA0). The protein complex was prepared for docking studies using protein preparation wizard in the Maestro interface (v11.1, Schrödinger, 2017). During the preparation process, it was observed that some amino acid residues in Chain A (37 to 47) and Chain B (275 to 284) were found missing along with hydrogen atoms in the protein complex. By employing homology-based modeling, the missing amino acid residues from Chain A and Chain B were rebuilt using different templates such as PDB ID: 3DU7 (C-chain) and PDB ID: 3RYC (D-chain) respectively with Prime 3.0 [11]. In the subsequent steps, all the water molecules were removed following which correct bond orders were assigned, formal charges and orientation of various groups were fixed in the complex. The orientation of hydroxyl groups and amide groups of Asn, Gln and His were converted into the charged state. The amino acid flips were assigned and hydrogen bonds optimized iteratively. Non-hydrogen atoms were minimized until the average root mean square deviation reaches to 0.3Å. Schrödinger modules Glide, Prime, QSite, Liasion, and MacroModel were used for protein preparation [15]. The remodeled structure was energy minimized using Optimized potentials for liquid simulations for all atoms (OPLS-AA)-2005 force field with Polak-ribiere conjugate gradient (PRCG) algorithm. The overall quality of the remodeled and energy minimized complex was evaluated using PROCHECK [16, 17], ERRAT [18], VERIFY3D [19], etc and proceeded for the subsequent molecular docking studies.

Screening of Inhibitors

From the literature studies, it was found that the phytosterol inhibitor β-sitosterol has been tested for its anthelminthic [20] and anti-cancer [10] property against the bovine form of alpha/beta-tubulin heterodimer. While the former reported the anthelminthic activity of β-sitosterol isolated from rhizomes of *Hedychium spicatum*, the latter described the anti-cancer property of β-sitosterol through biochemical characterization and molecular dynamics simulations performed with alpha/beta-tubulin heterodimer. Based on these observations, small molecule compounds structurally similar to β-sitosterol were searched in structural databases such as PubChem, Binding and ChemBridge for molecular docking studies. Among the repositories, a considerable number of hits were found in PubChem and Binding databases. Following an extensive manual inspection, the common hits found in both the databases were filtered out and hits found unique alone were retrieved for further studies.

Ligand Preparation

By using the LigPrep (Version 2.9) module, the co-crystal colchicine inhibitor, β-sitosterol, and its derivatives were geometry optimized and energy minimized using OPLS-2005 force field with the Steepest Descent followed by Conjugate gradient protocol. An appropriate bond order for each structure was assigned using LigPrep. The LigPrep process to perform conversions, apply corrections, generate variations and optimize the structures as well as eliminate unwanted structures.

High Throughput Virtual screening

Along with β-sitosterol, all the chosen derivatives were screened against the previously calculated active site grid receptor of co-crystal inhibitor using Standard Precision

(SP) and Extra Precision (XP) modules (rigid docking) in the Glide 7.4 software. In both, the procedures, various parameters such as docking score, glide Energy, glide model and nonbonded interactions of the inhibitors with the active site residues were subjected for docking analysis. From the SP and XP results, along with β-sitosterol about 11 compounds were found to be the best possible inhibitors and hence further proceeded for Induced Fit Docking (Flexible docking) studies.

Induced Fit Docking

Induced Fit Docking (IFD) was carried out using GLIDE where inhibitor and protein were held flexible and protein side chains allowed conformational changes based on the inhibitor binding mode at the active site. IFD uses a hierarchical series of filters to search for possible locations of the inhibitor at the active site region of the receptor. The shape and properties of the receptor are represented on a grid by several different sets of fields that provide progressively more accurate scoring of the inhibitor poses. Poses that pass these initial screens enter into the final stage of the algorithm, which involves evaluation and minimization of a grid approximation to the OPLS-AA, non-bonded ligand-receptor interaction energy. Final scoring is carried out based on the energy-minimized poses where the best one was chosen among the screened conformational poses based on docking score, glide energy, glide emodel and hydrogen bond interactions.

ADME Prediction

Absorption, distribution, metabolism, and excretion (ADME) properties for the top-ranked inhibitors obtained from IFD were evaluated using the QikProp module (QikProp, 5.1 Schrödinger). QikProp predicts the physically significant descriptors and pharmaceutically relevant properties of organic molecules. The selected 12 inhibitors were neutralized before being used in normal mode QikProp analysis. The program predicts 44 properties for a single inhibitor with a detailed analysis of QPP_{MDCK}, $Qplog_{HERG}$, and QPP_{Caco}. The acceptability of the inhibitor was based on Lipinski's rule of five.

Toxicity Prediction

Based on Glide scoring functions the top-ranked inhibitors obtained from IFD were further subjected to toxicity (Tox) prediction using several online software. The Property Tox Checker (https://mcule.com/apps/toxicity-checker/) was employed for identifying the presence of toxic fragments in the inhibitors. Identification of deleterious functional groups such as nitro, aniline, and hydrazine was performed using Free ADME-Tox Filtering (FAF-Drugs) online tool [21].

Cell Line Cytotoxicity Prediction

Prediction of probable cytotoxicity effect of drug candidates against tumor and normal human cell lines aid in designing more potent anti-cancer inhibitors. This can be achieved by combining the *in silico* analysis of the cytotoxic effect of chemicals on different cell-lines together and analysis of the ligand-target interactions. Using the online web service Cell Line Cytotoxicity Predictor (CLC-Pred), cytotoxicity effects of the lead inhibitors on various types of cancer cell lines were predicted [22].

RESULTS

Remodeling of Alpha/Beta Tubulin Heterodimer

After retrieving the alpha/beta-tubulin heterodimer structure from the PDB database, as described earlier the missing amino acid residues from both the chains were remodeled using the 'Builder' tool from the Maestro interphase (Figure 1a).

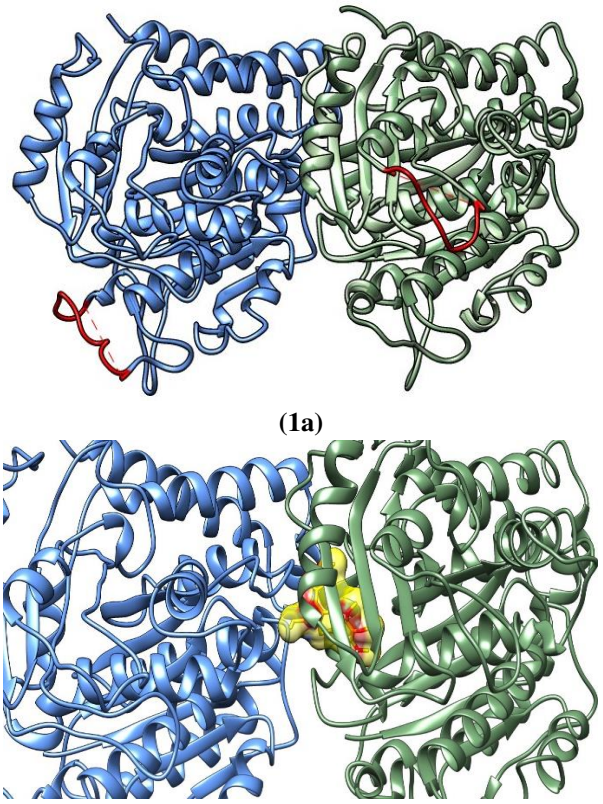

(1a)

(1b)

Fig.1a: Superimposed image of apo and remodeled Tubulin Heterodimer. The missing amino acid residues in both the chains and represented by loops in the rebuilt model are colored red. Fig.1b: Colchicine binding site (stick and surface) at the dimer interface. Chains A and B are colored Blue and Green respectively (cartoon).

Following this, the tubulin structure was energy minimized using the protein preparation wizard and further validated using several structure validation tools. Ramachandran Plot

obtained from PROCHECK results showed 94.4 % of backbone angles to be present in allowed region and 4.0 % residues in a generously allowed region with only 1.6 % residues found in the disallowed region. The overall quality factor as analyzed from the ERRAT calculator program and VERIFY 3D was found to be above 90 % indicating the precision of the alpha/beta-tubulin heterodimer has remained the same. The colchicine inhibitor binding site on tubulin has been considered as the active site pocket for several anticancer agents [9]. Therefore, in the present study, for all the docking procedures (SP, XP, and IFD) molecular interaction and binding affinity of β-sitosterol and its derivatives were tested on the colchicine binding site (Figure 1b).

High Throughput Virtual screening (HTVS)

As explained in the methodology section, the databases were filtered out for docking studies. Finally, along with β-sitosterol a total of 57 compounds confirmed to be unique were chosen for performing HTVS using SP and XP modules. All the compounds were redocked at the colchicine binding site following which their docking score, glide energy and hydrogen bonding interactions with the active site residues were analyzed. The best performed 12 compounds including β-sitosterol were taken for further flexible docking studies (Table 1).

Table 1: 2D Chemical Structure of Beta-Sitosterol and Lead Compounds

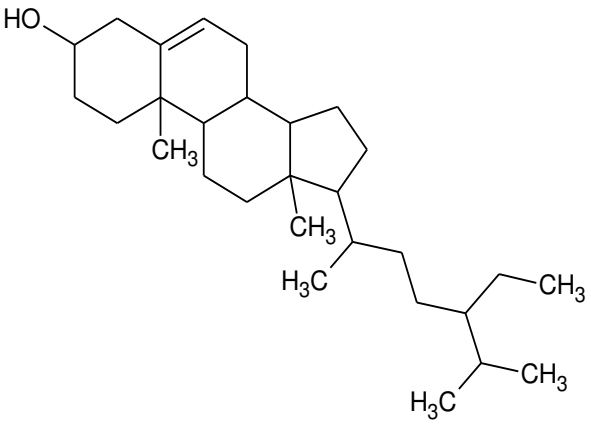

β-sitosterol

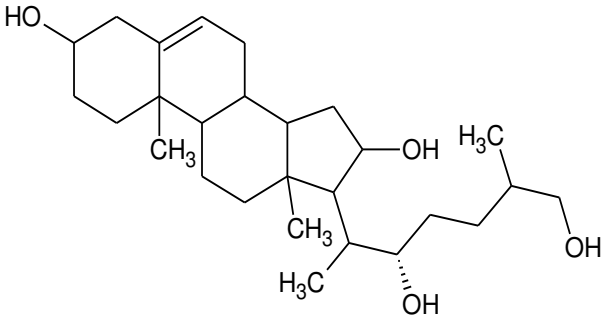

Compound 1

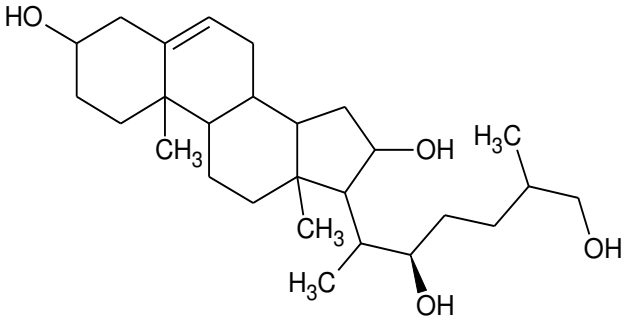

Compound 2

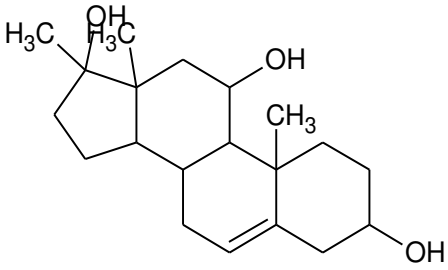

Compound 3

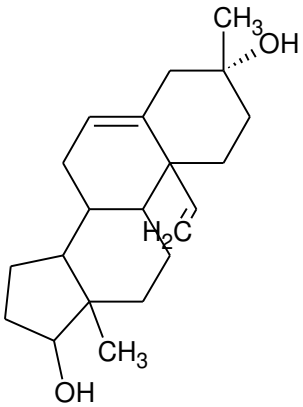

Compound 4

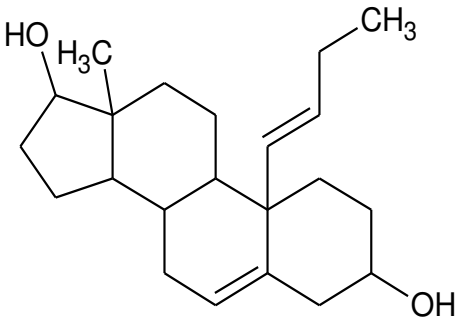

Compound 5

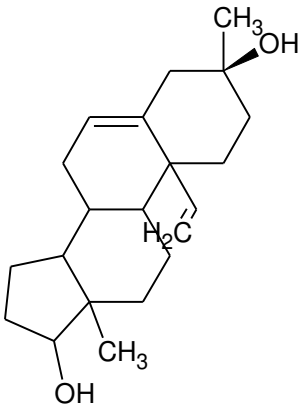

Compound 6

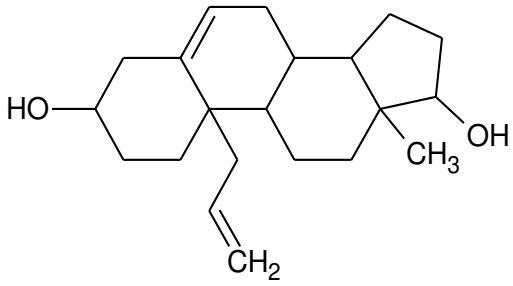

Compound 7

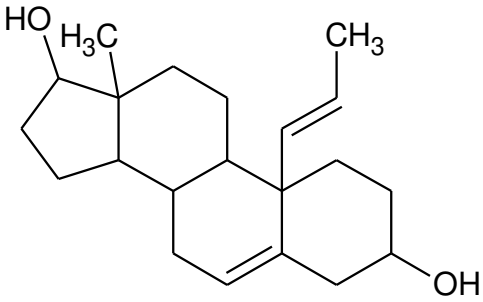

Compound 8

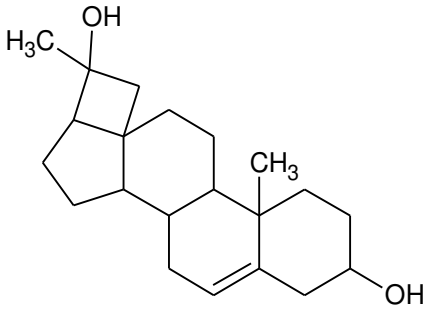

Compound 9

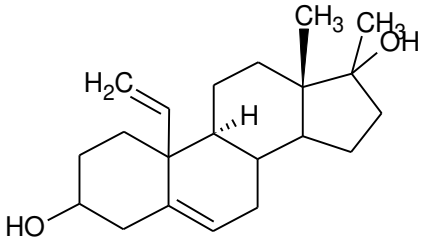

Compound 10

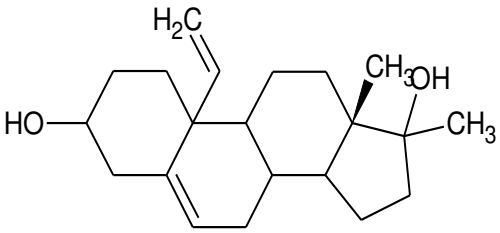

Compound 11

Induced Fit Docking

The accuracy of a docking procedure is normally evaluated by finding out how closely the lowest energy pose for a particular binding confirmation was predicted by the object scoring function. In most cases, the following three parameters are considered for predicting these results viz., docking score, glide energy and hydrogen bond interactions. The selected lead compounds were docked at the active site of the tubulin heterodimer and yielded a reliable docking score along with the hydrogen bonding interactions (Table 2, Figure 2a-2l). The IFD results showed that all the lead compounds have possessed glide score and energy in the range from -11.802 to -8.136 kcal/mol and -61.285 to -42.398 kcal/mol (Table 2), respectively. All the twelve compounds were involved in forming hydrogen bonding interactions with the active site key residues such as Asn 101, Thr 179 from A Chain and Val 238, Gln 247, Leu 248, Lys 254, Lys 352 from B Chain of the tubulin heterodimer. Based on the scoring function it was observed that three lead compounds have exhibited higher glide score and better energy than the chief compound β-sitosterol (Table 2).

Table 2: Induced Fit Docking Results of Beta-Sitosterol and Lead Compounds with Tubulin Heterodimer

Compound	Glide Score [kcal/mol]	Glide Energy [kcal/mol]	Glide EModel [kcal/mol]	H Bond Interactions D-H…A	Distance (Å)
β-sitosterol	-9.012	-46.157	-68.803	GLN 11 A N(E2)-H…O GLN 247 B N(E2)-H…O	3.0 3.2

Compound 1	-11.802	-61.285	-94.288	O-H…O VAL 238 B O-H…O LEU 248 B O-H…O LYS 254 B LYS 254 B N(Z)-H…O ASN 258 B N(D2)-H…O	2.7 2.7 2.8 3.3 2.7
Compound 2	-11.739	-59.786	-96.548	CYS 241 B N-H…O O-H…O VAL 238 B O-H…O LSY 254 B ASN 258 B N(D2)-H…O O-H…O ALA 317 B	3.4 2.7 2.9 3.0 3.2
Compound 3	-10.643	-50.857	-77.374	O-H…O VAL 238 B O-H…O(D1) ASN 258 B O-H…O LYS 352 B	2.6 2.8 2.7
Compound 4	-9.749	-51.998	-79.335	O-H…O LEU 248 B ALA 250 B N-H…O LYS 352 B N-H…O	2.9 3.2 3.1
Compound 5	-9.436	-42.969	-66.364	ASN 101 A N(D2)-H…O O-H…O VAL 315 B O-H…O LYS 352 B	2.9 3.3 3.1
Compound 6	-9.428	-47.77	-71.959	O-H…O THR 179 A LYS 352 B N(Z)-H…O	2.8 2.9
Compound 7	-9.325	-42.398	-64.289	ASN 101 A N(D2)-H…O O-H…O LYS 254 B ASN 258 B N(D2)-H…O O-H…O ALA 317 B	3.4 2.9 3.1 3.0
Compound 8	-9.134	-43.719	-65.375	ASN 101 A N(D2)-H…O O-H…O LYS 254 B O-H…O ALA 317 B	3.0 2.8 3.2
Compound 9	-9.093	-50.291	-76.882	O-H…O VAL 238 B	2.9
Compound 10	-8.827	-45.277	-68.918	O-H…O(D1) ASN 101 A O-H…O ALA 317 B	3.0 3.3
Compound 11	-8.136	-47.365	-70.830	O-H…O(D1) ASN 101 A LYS 352 B N(Z)-H…O	2.9 2.7

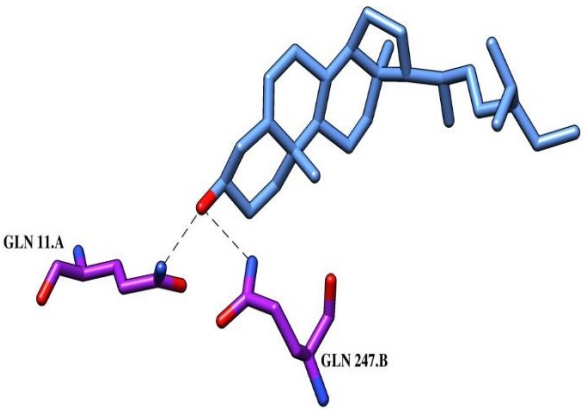

Fig.2a: β-sitosterol

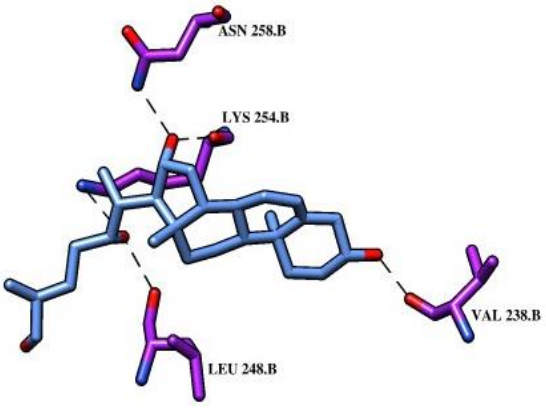

Fig.2b: Compound 1

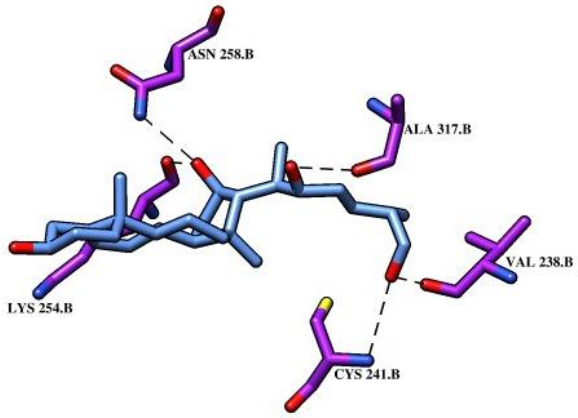

Fig.2c: Compound 2

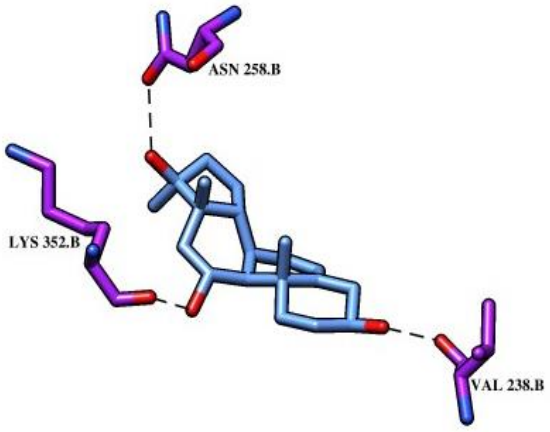

Fig.2d: Compound 3

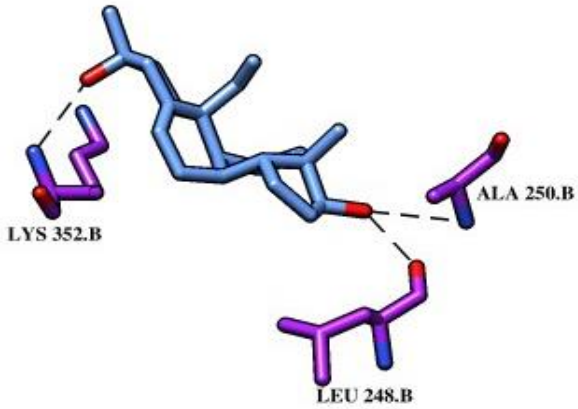

Fig.2e: Compound 4

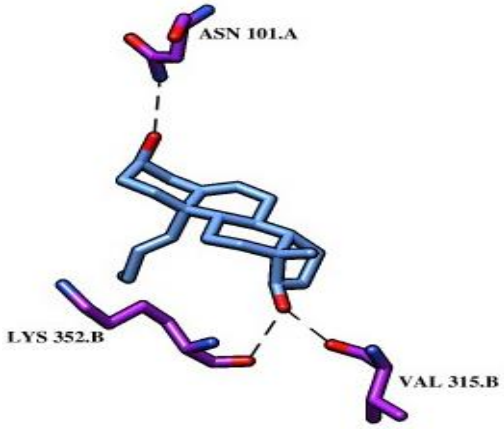

Fig.2f: Compound 5

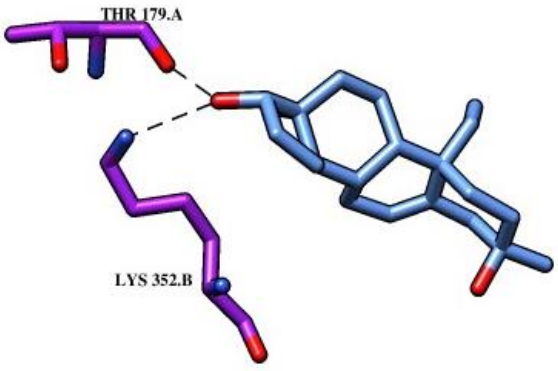

Fig.2g: Compound 6

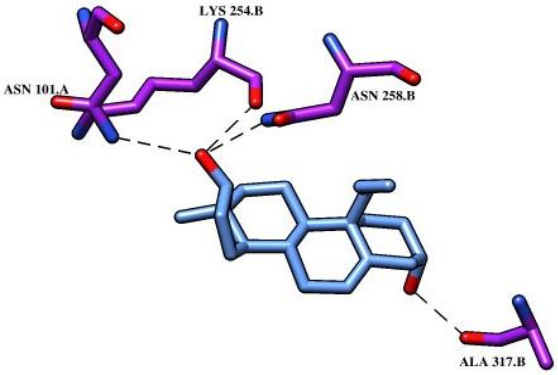

Fig.2h: Compound 7

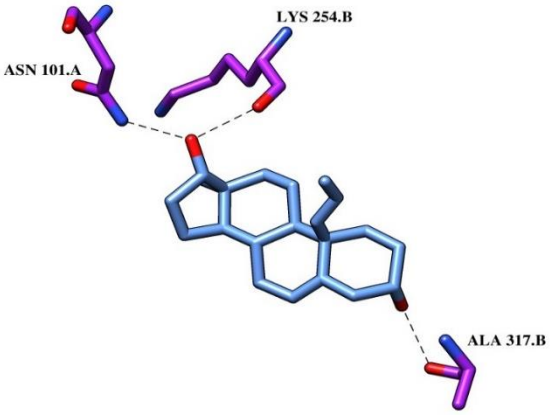

Fig.2i: Compound 8

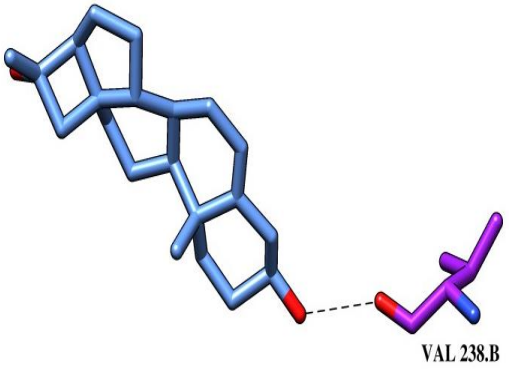

Fig.2j: Compound 9

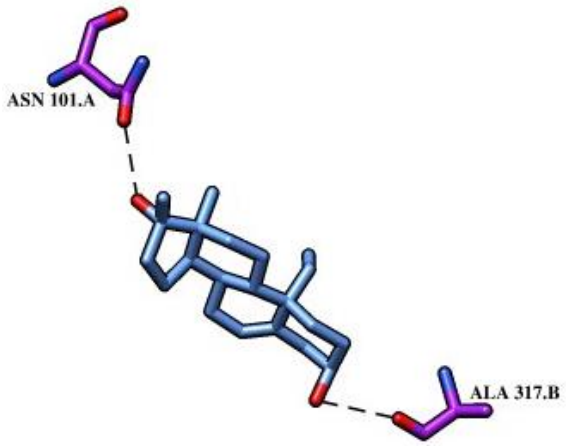

Fig.2k: Compound 10

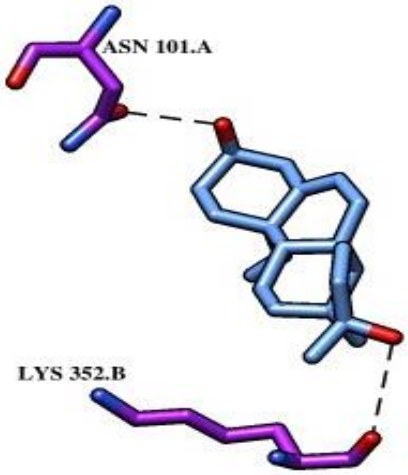

Fig.2l: Compound 11

Figures 2: Hydrogen Bond Interactions of Beta-Sitosterol and Lead Compounds (Cyan) with Active Site Residues (Purple) of Tubulin Heterodimer

ADME Evaluation

The selected twelve inhibitors were subjected to ADME prediction using the QikProp module and FAF-Drugs online tool. Many of these properties are essential for drug development and violation in any of these properties may result in delay or failure of the drug candidate to reach the market operation. Based on these criteria, several pharmacokinetic properties including molecular weight, some violations in Lipinski's rule of five, predicted octanol/water partition coefficient, etc were studied and presented in Table 3 and 4a-4b. As for the ADME results obtained from QikProp, it was found that all the twelve lead compounds have obeyed the Lipinski's rule of five. QPlogPw of the hits ranged from 12.725 to 3.375 whereas QPlogS ranged from -7.63 to -3.81 depicting that barring β-sitosterol the other lead compounds are found in the acceptable ADME range (Table 3).

Table 3: QikProp ADME Predictions of Beta-Sitosterol and Lead Compounds

S. No	Compounds	QPlogPw (4.0 to 45.0)	QPlogS (-6.5 to 0.5)	$QPlog_{HERG}$	QPP_{caco}	QPP_{MDCK}	Rule of five (Max 4)
1	β-sitosterol	3.375	-7.634	-3.999	3411.88	1864.03	0
2	Compound 1	12.724	-4.996	-4.021	523.66	245.858	0
3	Compound 2	12.725	-4.997	-4.022	523.43	245.741	0
4	Compound 3	9.611	-3.816	-2.99	791.27	384.107	0
5	Compound 4	6.201	-4.368	-2.904	1854.27	964.303	0
6	Compound 5	6.859	-4.96	-3.668	1836.19	954.145	0
7	Compound 6	6.178	-4.195	-2.689	1853.93	964.114	0
8	Compound 7	7.034	-4.284	-3.01	1466.56	748.346	0
9	Compound 8	6.923	-4.031	-2.836	1875.61	976.309	0
10	Compound 9	6.493	-4.805	-3.17	1661.36	856.341	0
11	Compound 10	6.152	-3.909	-2.33	1779.43	922.304	0
12	Compound 11	6.211	-4.348	-2.863	1778.95	922.035	0

Similarly, the ADME results fetched from the online tool FAF-drugs have shown that the molecular weight of all the lead compounds was within the accepted range of 315 to 440 Daltons (Table 4a). The number of hydrogen bond acceptors, as well as donors, were observed to be lesser than 5. The solubility index calculated for the lead compounds has revealed that β-sitosterol and compound 3 possessed the least and maximum solubility respectively (Table 4a). The oral bioavailability as estimated by VEBER and EGAN for the lead compounds was found to be "good" with none of them exhibited covalently binding property and pains (Table 4b).

Table 4a: FAF Drugs ADME Predictions of Beta-Sitosterol and Lead Compounds

Cmp ID	Mol.wt	logP	logD	logSw	tPSA	HB_D	HB_A	LR Violation	Solubility (mg/l)
β-sitosterol	414.71	9.34	7.84	-7.90	20.23	1	1	None	153.84
Compound 1	434.65	4.45	3.14	-4.94	80.92	4	4	None	3102.49
Compound 2	434.65	4.45	3.14	-4.94	80.92	4	4	None	3102.49
Compound 3	320.47	2.39	1.77	-3.33	60.69	3	3	None	11440.80
Compound 4	316.48	4.01	3.22	-4.26	40.46	2	2	None	4458.41
Compound 5	330.50	4.49	3.77	-4.59	40.46	2	2	None	3369.60
Compound 6	316.48	4.01	3.22	-4.26	40.46	2	2	None	4458.41
Compound 7	316.48	4.12	3.38	-4.27	40.46	2	2	None	4443.72
Compound 8	316.48	4.06	3.33	-4.29	40.46	2	2	None	4320.16
Compound 9	316.48	3.77	2.82	-4.18	40.46	2	2	None	4854.91
Compound 10	316.48	3.82	3.22	-4.14	40.46	2	2	None	5025.33
Compound 11	316.48	3.82	3.22	-4.14	40.46	2	2	None	5025.33

Mol.wt – Molecular weight (Daltons), HB_D – Hydrogen bond donor, HB_A – Hydrogen bond acceptor, LS – Lipinski's Rule

Table 4b: FAF Drugs ADME Predictions of Beta-Sitosterol and Lead Compounds

Cmp ID	OB (VEBER)	OB (EGAN)	SFI	Faf-Drugs		
				Pains	CI	Status
β-sitosterol	Good	Good	Reduced Solubility	None	None	Accepted
Compound 1	Good	Good	Good	None	None	Accepted
Compound 2	Good	Good	Good	None	None	Accepted
Compound 3	Good	Good	Good	None	None	Accepted
Compound 4	Good	Good	Good	None	None	Accepted
Compound 5	Good	Good	Good	None	None	Accepted
Compound 6	Good	Good	Good	None	None	Accepted
Compound 7	Good	Good	Good	None	None	Accepted
Compound 8	Good	Good	Good	None	None	Accepted
Compound 9	Good	Good	Good	None	None	Accepted
Compound 10	Good	Good	Good	None	None	Accepted
Compound 11	Good	Good	Good	None	None	Accepted

OB - Oral Bioavailability, SFI – Solubility Forecast Index, CI – Covalent Inhibitors

Toxicity Prediction

All 12 lead compounds were also subjected to toxicity prediction (Table 5). In most causes misinterpretation of ADMET properties in the identified hits fails in development and clinical trials. Computational toxicity prediction is a foremost vital process in the evaluation of hits before the experimental testing. Based on the toxicity results, among all the lead compounds, about five were found to be free of toxicity profiles. Incidentally, β-sitosterol was one among them with the top three compounds were also identified to be non-toxic (Table 5).

Table 5: Toxicity Prediction for Beta-Sitosterol and Lead Compounds

Cmp ID	Toxicity Checker
β-sitosterol	Non-Toxic
Compound 1	Non-Toxic
Compound 2	Non-Toxic
Compound 3	Non-Toxic
Compound 4	Toxic
Compound 5	Toxic
Compound 6	Toxic
Compound 7	Toxic
Compound 8	Toxic
Compound 9	Non-Toxic
Compound 10	Toxic
Compound 11	Toxic

CLC-Pred

The cytotoxicity effects exhibited by the lead compounds on tumor cell lines are presented in Table 6. From the results, it was deduced that while compounds 1, 2 and 7 exhibited activity only when the probability cut-off was set as P(a)ctive > P(i)nactive, the rest of the compounds

including β-sitosterol showed activity for the probability cut-off set at Pa > 0.5. Collectively, all the lead compounds were appeared to have cytotoxic effects on the various cell lines of gastric carcinoma, metastatic melanoma, glioblastoma, non-small cell lung cancer (stage 3), breast carcinoma and glioblastoma (Table 6).

Table 6: *In Silico* Prediction of Cytotoxic Effect of Beta-Sitosterol and Lead Compounds on Cancer Cell Lines

Compounds	Pa*	Pi*	Cell Line	Cell-Line Full Name	Tissue	Tumor Type
β-sitosterol$^{\phi}$	0.511	0.003	MKN-7	Gastric carcinoma	Stomach	Carcinoma
Compound 1 & 2$^{\Psi}$	0.494	0.033	SK-MEL-1	Metastatic melanoma	Skin	Melanoma
Compound 3$^{\phi}$	0.561	0.008	SF-539	Glioblastoma	Brain	Glioblastoma
Compound 4 & 6$^{\phi}$	0.630	0.016	NCI-H838	Non-small cell lung cancer. 3 stage	Lung	Carcinoma
Compound 5$^{\phi}$	0.573	0.037	MCF7	Breast carcinoma	Breast	Carcinoma
Compound 7$^{\Psi}$	0.486	0.037	SK-MEL-1	Metastatic melanoma	Skin	Melanoma
Compound 8$^{\phi}$	0.540	0.043	MCF7	Breast carcinoma	Breast	Carcinoma
Compound 9$^{\phi}$	0.506	0.029	SK-MEL-1	Metastatic melanoma	Skin	Melanoma
Compound 10 & 11$^{\phi}$	0.563	0.008	SF-539	Glioblastoma	Brain	Glioblastoma

*Pa - Probability to be Active, Pi - Probability to be Inactive, ϕ - (Pa > 0.50), Ψ - (Pa > Pi)

DISCUSSION

Detailed structural analysis of tubulin heterodimer has revealed that it consists of multiple binding sites such as colchicine, vinblastine, and taxol sites. Though most of the compounds are reported to bind either of these sites, compounds possessing anti-cancer properties are tested on the colchicine binding site [14]. Colchicine is found to bind tubulin with high affinity which makes them copolymerized forming microtubules. This results in the formation of curved tubulin dimer preventing them from adopting a straight structure. Although they are not considered or treated as an anticancer agent, efforts are being made to clinically develop colchicine binding site agents (CBSI) [14]. A major plant sterol, β-sitosterol is known to regulate blood cholesterol levels [23] and also possess anti-atherogenic [24], anti-diabetic [19], and anti-asthmatic [25] properties.

Several studies describing the effects of β-sitosterol on microtubules are previously reported. In particular, Mahaddalkar *et al* described the anticancer properties of β-sitosterol through biochemical characterization indicating that it could be developed into a potent anticancer drug [26]. A report by Moon *et al*. (2008) indicated that the sterol can arrest cells at G2/M and affect microtubule assembly [27]. Considering the current drawbacks of existing anticancer drugs, β-sitosterol emerged as a promising anti-cancer agent. In this context, in the present study attempts were made to carry out molecular docking on tubulin heterodimer using β-sitosterol and its derivatives obtained from various databases. The protein structure was prepared as reported earlier following which molecular docking was performed with β-sitosterol derivatives. To choose the best possible inhibitors, all the compounds were subjected to rigid docking using SP and XP mode. At the end of these procedures, compounds that exhibited higher glide score and energy with a reliable number of hydrogen bonding interactions were analyzed and retrieved separately. In the process, about 12 compounds including β-sitosterol were found to be the best possible inhibitors satisfying the above-mentioned parameters and hence were subjected for further IFD analysis. The IUPAC name of 12 compounds is provided in Appendix 1.

The IFD results showed that all the lead inhibitors were found to bind at the interface of tubulin heterodimer (i.e. colchicine binding site). This was following the findings reported by Das *et al* and Bajarang *et al* where the dimer interface remained the preferred binding site for the respective lead compounds described in their study [12, 13]. The lead inhibitors were involved in hydrogen bonding interactions with the following residues Val 238, Cys 241, Gln 247, Leu 248, Ala 250, Lys 254, Asn 258, Val 315, Ala 317, Lys 352 from B Chain and Gln 11, Asn 101, Thr 179 from A Chain (Figure 2a-2l). Based on their docking score and energy, compounds 1 and 2 are considered to be the most potent inhibitors possessing a docking score of -11.802 and -11.739 respectively. Similarly, their corresponding glide energy was also found to be higher with values of -61.285 and -59.786 kcal/mol respectively (Table 2). Though the chief inhibitor β-sitosterol exhibited a relatively lesser dock score (-9.012) and glide energy (-46.157), still it was found involved in hydrogen bonding interactions with residues of both subunits (Table 2, Figure 2a). The other leads such as inhibitor 5, 6, 7 and 8 were also seen exhibiting hydrogen bonding interactions with residues of both subunits (Table 2, Figure 2f-2i). Using QikProp and FAF-Drugs the ADME properties of all the lead compounds were evaluated. Among the tested lead inhibitors only for β-sitosterol, parameters related to lipophilicity such QPlogS (Table 3) and logP (Table 4a) were observed with values

higher than the acceptable range. As for the other parameters all the values were found within the admissible range (Table 3 and Table 4a). For the other lead inhibitors apart from satisfying all the parameters, it was also observed that none of them possessed either the property of "covalently binding to the protein" or capable of inducing "pains". Most of the compound's oral bioavailability and solubility forecast index were predicted as "good" (Table 4b).

The available toxic fragments in the lead inhibitors were predicted using online web service "mcule" (https://mcule.com/apps/toxicity-checker). The results showed that along with β-sitosterol the top-ranked 3 lead inhibitors 1, 2 and 3 (based on their glide scoring functions) were found to be free of toxic fragments (Table 5). Apart from these 4 leads, inhibitor 9 with a glide score and energy of -9.093 and -50.291 respectively was also found to be free of toxic fragments (Table 5). The possible cytotoxicity effects that can be exhibited by the lead inhibitors on tumor cell lines were computed using the CLC-Pred online tool. Most of the inhibitors showed significant cytotoxicity property on various cancer cell lines with "Pa" (probability to be active) value of greater than 0.5 (Table 6). In particular, inhibitors 4 and 6 possessed the highest "Pa" value of 0.63 on the tumor cell line NCI-H838 belonging to non-small cell lung carcinoma. The next best was found to be compound 5 which showed a "Pa" value of 0.57 on the cell line MCF7 representing the breast carcinoma (Table 6). The chief compound β-sitosterol exhibited a relatively higher "Pa" value of 0.51 on the cell line MKN-7 belonging to gastric carcinoma (Table 6). All the other lead inhibitors exhibited "Pa" value in the range of 0.56-0.49 on different cell lines such as SF-539, MCF7 and SK-MEL-1 of glioblastoma, breast carcinoma and metastatic melanoma tumors respectively (Table 6).

In the work done by Manchukonda *et al*, 'noscapine' a phthalide isoquinoline and its analogs were examined for its potency as tubulin-binding agents. They have reported that among the several synthesized analogs, a specific compound was identified to possess a higher apoptotic index on MCF7 cell lines belonging to breast carcinoma [11]. A similar kind of result was observed in the present study also were one of the top-ranked hits (compound 5) exhibited significant cytotoxicity effect on the MCF7 cell line (Table 6). Overall, the lead compounds, β-sitosterol, and its derivatives possess great potential for designing potent anti-cancer compounds that can be used in further preclinical and clinical evaluation.

CONCLUSION

It has been well established that β-sitosterol exhibits functional biochemical similarities with existing drugs such as Taxol and Taccalonolides. When used in combination, these inhibitors are known to suppress the dynamic instability of microtubule without inhibiting their polymer mass leading to mitotic arrest and cell death [28-30]. Based on the several published works, in the present study attempts were made to evaluate the anti-cancer property of β-sitosterol and its derivatives using molecular docking and ADME properties. For this, the crystal structure of bovine alpha/beta-tubulin heterodimer was retrieved and the colchicine binding site at the dimer interface was chosen as the preferred binding site. By employing rigid docking, most of the inhibitors were filtered out and along with β-sitosterol, about twelve inhibitors were subjected for IFD studies. From the docking results, it was found evidence that all the compounds have shown reliable docking scores and energy forming hydrogen bonding interactions with the key residues of both the subunits. Evaluation of ADME parameters has revealed that the lead compounds satisfied most of the properties required to retain the "drug-likeness" quality. While the top-ranked compounds and β-sitosterol showed no presence of toxic fragments few compounds involved in hydrogen bonding interactions with residues of both subunits have possessed traces of toxic fragments. *In silico* predictions of cytotoxicity effects have showed that all the lead compounds exhibited profound cytotoxicity with "Pa" value in the range of 0.63-0.49 on different cell lines such as MKN-7 (gastric carcinoma), SK-MEL-1 (metastatic melanoma), SF-539 (glioblastoma), NCI-H838 (non-small cell lung cancer) and MCF7 (breast carcinoma). To summarise, the present computational study provides a detailed understanding of the molecular interactions of β-sitosterol and its derivatives with tubulin heterodimer. The combined molecular modeling results provide insights for designing more potent β-sitosterol analogs with reduced or less toxicity which can be further utilized in treating patients with advanced carcinomas.

ACKNOWLEDGMENT

This work was supported by the National Institute of Science and Technology -Biorational Control of Insects and Pests (INCT-CBIP; grant numbers FAPESP 2008/51859-5 and CNPq 573742/2008-1), São Paulo State Foundation for Research (FAPESP; grant numbers 2018/00492-4. The authors would also like to thank Prof. R.S. Neelakandan, Prof. T. Kannan, Prof. Dr. Andre Luis Berteli Ambrosio and Prof. Dr. Rafael Victório Carvalho Guido for research support and software facility.

Conflict of interest

Nil.

REFERENCES

[1] Saha SK, Khuda-Bukhsh AR. Molecular approaches towards development of purified natural products and their structurally known derivatives as efficient anti-cancer drugs: current trends. European journal of pharmacology. 2013 Aug 15;714(1-3):239-48.

[2] Bhat SH, Ullah MF, Abu-Duhier FM. Anti-hemolytic Activity and Antioxidant Studies of Caralluma quadrangula: Potential for Nutraceutical Development in Cancers and Blood Disorders. International Journal of Pharmaceutical Research & Allied Sciences, 2019;8(4):121-9.

[3] Al-Harbi NA, Awad NS, Alsberi HM, Abdein MA. Apoptosis Induction, Cell Cycle Arrest and in Vitro Anticancer Potentiality of Convolvulus Spicatus and Astragalus Vogelii. World. 2019;8(4):69-75.

[4] Sivak E, Bugaev S, Sokolov M, Glinushkin A. Antimicrobial Bio-Components from Red Algae Species: a Review of Application and Health Benefits. Entomology and Applied Science Letters. 2018 Sep 30;5(3):85-90.

[5] Jiménez-Escrig A, Santos-Hidalgo AB, Saura-Calixto F. Common sources and estimated intake of plant sterols in the Spanish diet. Journal of agricultural and food chemistry. 2006 May 3;54(9):3462-71.

[6] Yuniarto A, Sukandar EY, Fidrianny I, Setiawan F, Ketut I. Antiobesity, Antidiabetic and Antioxidant Activities of Senna (Senna alexandrina Mill.) and Pomegranate (Punica granatum L.) Leaves Extracts and Its Fractions. International Journal of Pharmaceutical and Phytopharmacological Research (eIJPPR). 2018 Jun 1;8(3):18-24.

[7] Awad AB, Chen YC, Fink CS, Hennessey T. beta-Sitosterol inhibits HT-29 human colon cancer cell growth and alters membrane lipids. Anticancer research. 1996;16(5A):2797-804.

[8] v von Holtz RL, Fink CS, Awad AB. β-sitosterol activates the sphingomyelin cycle and induces apoptosis in LNCaP human prostate cancer cells. Nutr Cancer, 1998; 32, pp.8-12.

[9] Baskar AA, Ignacimuthu S, Paulraj GM, Al Numair KS. Chemopreventive potential of β-sitosterol in experimental colon cancer model-an in vitro and in vivo study. BMC complementary and alternative medicine. 2010 Dec 1;10(1):24.

[10] Mahaddalkar T, Suri C, Naik PK, Lopus M. Biochemical characterization and molecular dynamic simulation of β-sitosterol as a tubulin-binding anticancer agent. European journal of pharmacology. 2015 Aug 5;760:154-62.

[11] Manchukonda NK, Naik PK, Santoshi S, Lopus M, Joseph S, Sridhar B, Kantevari S. Rational design, synthesis, and biological evaluation of third generation α-noscapine analogues as potent tubulin binding anti-cancer agents. PloS one. 2013;8(10):1-17.

[12] Das L, Gupta S, Dasgupta D, Poddar A, Janik ME, Bhattacharyya B. Binding of indanocine to the colchicine site on tubulin promotes fluorescence, and its binding parameters resemble those of the colchicine analogue AC. Biochemistry. 2009 Feb 24;48(7):1628-35.

[13] Kumbhar BV, Panda D, Kunwar A. Interaction of microtubule depolymerizing agent indanocine with different human αβ tubulin isotypes. PloS one. 2018;13(3):1-20.

[14] Lu Y, Chen J, Xiao M, Li W, Miller DD. An overview of tubulin inhibitors that interact with the colchicine binding site. Pharmaceutical research. 2012 Nov 1;29(11):2943-71.

[15] Halgren TA, Murphy RB, Friesner RA, Beard HS, Frye LL, Pollard WT, Banks JL. Glide: a new approach for rapid, accurate docking and scoring. 2. Enrichment factors in database screening. Journal of medicinal chemistry. 2004 Mar 25;47(7):1750-9.

[16] Laskowski RA, MacArthur MW, Moss DS, Thornton JM. PROCHECK: a program to check the stereochemical quality of protein structures. Journal of applied crystallography. 1993 Apr 1;26(2):283-91.

[17] Ramachandran GN. Stereochemistry of polypeptide chain configurations. J. Mol. Biol.. 1963;7:95-9.

[18] Colovos C, Yeates TO. Verification of protein structures: patterns of nonbonded atomic interactions. Protein science. 1993 Sep;2(9):1511-9.

[19] Eisenberg D, Lüthy R, Bowie JU. [20] VERIFY3D: assessment of protein models with three-dimensional profiles. InMethods in enzymology 1997 Jan 1 (Vol. 277, pp. 396-404). Academic Press.

[20] Sravani T, Paarakh PM, Shruthi SD. In silico and in vitro anthelmintic activity of β-sitosterol isolated from rhizomes of Hedychium spicatum Buch.-Ham. Indian Journal of Natural Products and Resources, 5(3), pp.258-261.

[21] Lagorce D, Sperandio O, Galons H, Miteva MA, Villoutreix BO. FAF-Drugs2: free ADME/tox filtering tool to assist drug discovery and chemical biology projects. BMC bioinformatics. 2008 Dec;9(1):396.

[22] Lagunin AA, Dubovskaja VI, Rudik AV, Pogodin PV, Druzhilovskiy DS, Gloriozova TA, Filimonov DA, Sastry NG, Poroikov VV. CLC-Pred: a freely available web-service for in silico prediction of

human cell line cytotoxicity for drug-like compounds. PloS one. 2018;13(1):1-13.

[23] Wu AH, Ruan W, Todd J, Lynch KL. Biological variation of β-sitosterol, campesterol, and lathosterol as cholesterol absorption and synthesis biomarkers. Clinica chimica acta. 2014 Mar 20;430:43-7.

[24] Rosenblat M, Volkova N, Aviram M. Pomegranate phytosterol (β-sitosterol) and polyphenolic antioxidant (punicalagin) addition to statin, significantly protected against macrophage foam cells formation. Atherosclerosis. 2013 Jan 1;226(1):110-7.

[25] Yuk JE, Woo JS, Yun CY, Lee JS, Kim JH, Song GY, Yang EJ, Hur IK, Kim IS. Effects of lactose-β-sitosterol and β-sitosterol on ovalbumin-induced lung inflammation in actively sensitized mice. International immunopharmacology. 2007 Dec 5;7(12):1517-27.

[26] Lamiaa ML, Eman SA. The Impact of Pomegranate Peel-fortified Cupcakes on Weight Loss. International Journal of Pharmaceutical Research & Allied Sciences. 2019 Jul 1;8(3).

[27] Moon DO, Kim MO, Choi YH, Kim GY. β-Sitosterol induces G2/M arrest, endoreduplication, and apoptosis through the Bcl-2 and PI3K/Akt signaling pathways. Cancer letters. 2008 Jun 18;264(2):181-91.

[28] Madari H, Panda D, Wilson L, Jacobs RS. Dicoumarol: a unique microtubule stabilizing natural product that is synergistic with Taxol. Cancer research. 2003 Mar 15;63(6):1214-20.

[29] Risinger AL, Li J, Bennett MJ, Rohena CC, Peng J, Schriemer DC, Mooberry SL. Taccalonolide binding to tubulin imparts microtubule stability and potent in vivo activity. Cancer research. 2013 Nov 15;73(22):6780-92.

[30] Risinger AL, Riffle SM, Lopus M, Jordan MA, Wilson L, Mooberry SL. The taccalonolides and paclitaxel cause distinct effects on microtubule dynamics and aster formation. Molecular cancer. 2014 Dec 1;13(1):41.

[31] Radika MK, Viswanathan P, Anuradha CV. Nitric oxide mediates the insulin sensitizing effects of β-sitosterol in high fat diet-fed rats. Nitric Oxide. 2013 Aug 1;32:43-53.

APPENDIX 1

Compounds used in IFD	IUPAC NAME
β-sitosterol	(3S,8S,9S,10R,13R,14S,17R)-17-[(2R,5R)-5-ethyl-6-methylheptan-2-yl]-10,13-dimethyl-2,3,4,7,8,9,11,12,14,15,16,17-dodecahydro-1H-cyclopenta[a]phenanthren-3-ol
Compound 1	(3S,8S,9S,10R,13S,14S,16S,17R)-17-[(2S,3S,6R)-3,7-dihydroxy-6-methylheptan-2-yl]-10,13-dimethyl-2,3,4,7,8,9,11,12,14,15,16,17-dodecahydro-1H-cyclopenta[a]phenanthrene-3,16-diol
Compound 2	(3S,8S,9S,10R,13S,14S,16S,17R)-17-[(2S,3R,6R)-3,7-dihydroxy-6-methylheptan-2-yl]-10,13-dimethyl-2,3,4,7,8,9,11,12,14,15,16,17-dodecahydro-1H-cyclopenta[a]phenanthrene-3,16-diol
Compound 3	(3S,8S,9S,10R,11S,13S,14S,17S)-10,13,17-trimethyl-1,2,3,4,7,8,9,11,12,14,15,16-dodecahydrocyclopenta[a]phenanthrene-3,11,17-triol
Compound 4	(3R,8R,9S,10S,13S,14S,17S)-10-ethenyl-3,13-dimethyl-1,2,4,7,8,9,11,12,14,15,16,17-dodecahydrocyclopenta[a]phenanthrene-3,17-diol
Compound 5	(3S,10S,13S,17S)-10-[(Z)-but-1-enyl]-13-methyl-2,3,4,7,8,9,11,12,14,15,16,17-dodecahydro-1H-cyclopenta[a]phenanthrene-3,17-diol
Compound 6	(3S,8R,9S,10S,13S,14S,17S)-10-ethenyl-3,13-dimethyl-1,2,4,7,8,9,11,12,14,15,16,17-dodecahydrocyclopenta[a]phenanthrene-3,17-diol
Compound 7	(3S,10S,13S,17S)-13-methyl-10-prop-2-enyl-2,3,4,7,8,9,11,12,14,15,16,17-dodecahydro-1H-cyclopenta[a]phenanthrene-3,17-diol
Compound 8	(3S,10S,13S,17S)-13-methyl-10-[(E)-prop-1-enyl]-2,3,4,7,8,9,11,12,14,15,16,17-dodecahydro-1H-cyclopenta[a]phenanthrene-3,17-diol
Compound 9	(1S,2S,5S,8R,11S,12R,15S)-6,12-dimethylpentacyclo [9.8.0.$0^{2,8}$.$0^{5,8}$.$0^{12,17}$]nonadec-17-ene-6,15-diol
Compound 10	(3S,8R,9S,10S,13S,14S,17S)-10-ethenyl-13,17-dimethyl-1,2,3,4,7,8,9,11,12,14,15,16-dodecahydrocyclopenta[a]phenanthrene-3,17-diol
Compound 11	(3S,10S,13S,17S)-10-ethenyl-13,17-dimethyl-1,2,3,4,7,8,9,11,12,14,15,16-dodecahydrocyclopenta[a]phenanthrene-3,17-diol